



Radiogenomics Map Reveals the Landscape of m6A Methylation Modification Pattern in Bladder Cancer

Fangdie Ye^{1,2†}, Yun Hu^{1,2†}, Jiahao Gao^{3†}, Yingchun Liang^{1,2}, Yufei Liu^{1,2}, Yuxi Ou^{1,2}, Zhang Cheng^{1,2} and Haowen Jiang^{1,2,4*}

OPEN ACCESS

Edited by:

Wei Wei,
Institute for Systems Biology (ISB),
United States

Reviewed by:

Xiaopan Xu,
Fourth Military Medical University,
China
Yuanshen Zhao,
Chinese Academy of Sciences (CAS),
China
Dachun Zhao,
Peking Union Medical College Hospital
(CAMS), China

*Correspondence:

Haowen Jiang
urology_hs@163.com

[†]These authors have contributed
equally to this work

Specialty section:

This article was submitted to
Cancer Immunity
and Immunotherapy,
a section of the journal
Frontiers in Immunology

Received: 09 June 2021

Accepted: 30 September 2021

Published: 18 October 2021

Citation:

Ye F, Hu Y, Gao J, Liang Y, Liu Y, Ou Y,
Cheng Z and Jiang H (2021)
Radiogenomics Map Reveals
the Landscape of m6A
Methylation Modification
Pattern in Bladder Cancer.
Front. Immunol. 12:722642.
doi: 10.3389/fimmu.2021.722642

¹ Department of Urology, Huashan Hospital, Fudan University, Shanghai, China, ² Fudan Institute of Urology, Huashan Hospital, Fudan University, Shanghai, China, ³ Department of Radiology, Huashan Hospital, Fudan University, Shanghai, China, ⁴ National Clinical Research Center for Aging and Medicine, Huashan Hospital, Fudan University, Shanghai, China

We aimed to develop a noninvasive radiomics approach to reveal the m6A methylation status and predict survival outcomes and therapeutic responses in patients. A total of 25 m6A regulators were selected for further analysis, we confirmed that expression level and genomic mutations rate of m6A regulators were significantly different between cancer and normal tissues. Besides, we constructed methylation modification models and explored the immune infiltration and biological pathway alteration among different models. The m6A subtypes identified in this study can effectively predict the clinical outcome of bladder cancer (including m6AClusters, geneClusters, and m6AScore models). In addition, we observed that immune response markers such as PD1 and CTLA4 were significantly correlated with the m6AScore. Subsequently, a total of 98 obtained digital images were processed to capture the image signature and construct image prediction models based on the m6AScore classification using a radiomics algorithm. We constructed seven signature radiogenomics models to reveal the m6A methylation status, and the model achieved an area under curve (AUC) degree of 0.887 and 0.762 for the training and test datasets, respectively. The presented radiogenomics models, a noninvasive prediction approach that combined the radiomics signatures and genomics characteristics, displayed satisfactory effective performance for predicting survival outcomes and therapeutic responses of patients. In the future, more interdisciplinary fields concerning the combination of medicine and electronics remains to be explored.

Keywords: m6A, radiogenomics, contrast-enhanced computed tomography, immunotherapy, mutation burden

INTRODUCTION

The whole genome distribution of N⁶-Methyladenosine (m6A) was not revealed until 2012; it is the most common epigenetic modification of the eukaryotic transcriptome, affecting almost every process of RNA metabolism, including translation, folding, splicing, degradation, and export (1–5). m6A RNA methylation is a reversible and dynamic procedure, which is catalyzed by the m6A

methyltransferase complex consisting of methyltransferases (writers), including VIRMA, WTAP, METTL3/14/15/16, RBM15, RBM15B, and ZC3H13. Among the m6A RNA methyltransferase complexes, METTL3 is the key component (6, 7). The m6A modification is removed by demethylases (erasers), including ALKBH5 and FTO (8, 9). Fourteen binding proteins act as “readers,” which specifically recognize the m6A modification and produce m6A modified RNA, including ELAVL1, FMR1, HNRNPA2B1, HNRNPC, IGF2BP1/2/3, LRPPRC, RBMX, YTHDC1/2, and YTHDF1/2/3 (10, 11). An increasing number of studies have found that m6A modification is involved in a variety of biological processes, including embryonic development disorders, tumor development, and immune cell infiltration (12–14). Notably, the imbalance of m6A modification is significantly associated with the occurrence and progression of various cancers, such as bladder cancer, pancreatic cancer, hepatocellular carcinoma, and colorectal cancer (15–18). In brief, m6A modification plays a role in carcinogenesis and tumor inhibition in diverse scenarios.

Recent progress in genetics has allowed for extensive genomics and transcriptome analyses to reveal the potential molecular mechanism underlying bladder cancer. Radiomics, another new technology, has enabled the identification of significant imaging signatures that could not be captured by the unaided eye and the exploitation of the potential characteristics of digital imaging. Radiomics can transform biomedical images into mineable quantitative characteristics, and then conduct subsequent analyses to improve the effective performance of preoperative expectation, tumor classification, prognosis prediction, and treatment response (19–21). Radiogenomics is an emerging cross-disciplinary study between radiomics and genomics, which is the simplest method used to extract high-level genomic information. In recent years, it has been extended to connect radiomics with broader biological characteristics, such as proteomics and metabolomics (22, 23). Previous studies have explored tumor gene expression, tumor mutation burden, methylation pattern, and subtypes using non-invasive digital imaging features (24–26). In addition, a combination of radiomics and genomics can contribute to improving the efficiency of clinical prediction in some cancers (27, 28). Thus, radiogenomics may help us understand the molecular phenotype of various cancers and provide real-time monitoring for the clinical management of individual patients.

Bladder cancer is the sixth most common cancer and the ninth most common cause of cancer death among males worldwide; a highly malignant urogenital tumor characterized by hidden onset and easy misdiagnosis (29). Distinct proportions of genome subclones lead to cellular and molecular heterogeneity in this type of tumor, which affects both clinical outcomes and therapeutic responses (30, 31). Cystoscopy, as a traditional diagnostic technology, is restricted in realizing the purpose of individualized medicine because of the inability to identify genome subclones, and it is an invasive method. Thus, increasing studies have begun to focus on image processing to help predict the clinical outcomes of Bca patients. Xu X. et al.

systematically retrieved the research reports on the application of radiomics in bladder cancer from 2000 to 2021, described the current blueprint of this field for researches, and comprehensively explained its pitfalls, challenges and opportunities (32). Xu S. et al. also combined with diffusion-weighted imaging (DWI) radiomics features and clinical data of transurethral resection to improve the sensitive and accuracy for the detection of muscle invasive bladder cancer (33). Therefore, it is imperative to develop a new non-invasive technology to help clinicians make correct judgement and reduce unnecessary invasive examinations.

In this study, we aimed to develop a noninvasive radiomics approach to reveal the m6A methylation status and predict survival outcomes of Bca patients. We collected the Genomic data from 716 cases of bladder cancer, and then construct the methylation modification pattern by unsupervised clustering of m6A regulators expression level. We investigated the expression of m6A regulators rather than m6A methylation itself, as the biological function of m6A methylation will alter based on genomic context. Three distinct m6A methylatin modification patterns with different tumor microenviroment were identified. In the final analysis of genomics, we identified m6A-related prognostic genes, and constructed the m6AScore system based on the expression levels of these genes to quantify the m6A methylation status of individual samples. As for the radiomics, a total of 120 samples had complete digital images were obtained from the Cancer Imaging Archive (TCIA) database. We used a radiomics algorithm to obtain the image signature and constructed image prediction models based on the m6AScore system classification. In brief, our findings revealed the critical role of m6A RNA methylation in bladder cancer, and we proposed a convenient method to help diagnose and predict the survival outcomes of patients with bladder cancer.

METHODS

Data Acquisition of Bladder Cancer Samples

The transcriptome data and adjusted clinical information of bladder cancer samples were retrospectively acquired from the Gene Expression Omnibus (GEO) and The Cancer Genome Atlas (TCGA) databases. A total of 716 samples were selected for analysis, including those from the Cancer Genome Atlas Urothelial Bladder Carcinoma (TCGA-BLCA) database ($n = 408$) and GSE32894 dataset ($n = 308$). Transcriptome data and genomic mutation data of the TCGA-BLCA were obtained from the UCSC Xena database. The m6A regulators were collected based on several articles, including nine methyltransferases (writers; VIRMA, WTAP, METTL3/14/15/16, RBM15, RBM15B, and ZC3H13), two demethylases (erasers; ALKBH5 and FTO), and 14 binding proteins (readers; ELAVL1, FMR1, HNRNPA2B1, HNRNPC, IGF2BP1/2/3, LRPPRC, RBMX, YTHDC1/2, YTHDF1/2/3) (34–37). The effective clinical immunotherapy performance and digital imaging information of bladder cancer were obtained from the Cancer Imaging Archive (TCIA) database.

Unsupervised Clustering of Twenty-Five m6A Regulators

To determine the distinct m6A modification patterns mediated by m6A regulators, unsupervised consensus clustering analysis was performed based on the expression level of the 21 identified m6A regulators (4 identified m6A regulators were excluded due to missing GSE32894 transcriptome data). Principal component analysis (PCA) was performed to determine whether each subtype was relatively independent of the others. The R package “consensusClusterPlus” was utilized to determine the cluster count, and 1000 repetitions and $p_{\text{tem}}=0.8$ were executed to verify the stability of the subtype. The R package “gene set variation analysis (GSVA)” was then used to assess any differences in biological pathways among subtypes (38). The identified biological features were obtained from the Kyoto Encyclopedia of Genes and Genomes (KEGG) database (39).

Immune Cell Infiltration and Tumor Mutation Burden Estimation

Single-sample gene set enrichment analysis (ssGSEA) is designed for analysis of a single sample that could not be processed using standard GSEA (40). The relative abundance of immune cells in bladder cancer was estimated by performing ssGSEA based on the expression levels of immune cell-related genes (41). The deconvolution algorithm “cibersort” was then employed to assess the relative abundance of 22 infiltration immune cells and the “ESTIMATE” algorithm was applied to calculate the stromal and immune abundance based on the RNA-seq data of bladder cancer. We also used the “MutSigCV” algorithm to select oncogenes with a higher mutation frequency than the background. The mutation landscapes of oncogenes and m6A regulators in TCGA-BLCA cohort were displayed using the R package “maftools.”

Selection of m6A Prognostic Related Genes Between Diverse Subtypes

To select the m6A related genes, the empirical Bayesian function of the R package “limma” was employed to select the differentially expressed genes (DEGs) among diverse subtypes, which we termed m6A related genes. The adjusted p value was 0.001. We then adopted univariate Cox regression analysis to extract the m6A prognostic related genes for further analysis. To prove that m6A prognostic-related genes (MPRGs) play an important role in tumor progression, we classified tumor samples into diverse gene clusters by employing an unsupervised clustering method according to the MPRGs expression levels.

Construction of m6AScore Models

The above models were only based on the patient population and cannot accurately predict the m6A methylation status of an individual patient. Therefore, we designed an m6AScore to assess the m6A modification patterns of individual samples. Based on the m6A prognostic-related gene expression level, we constructed the m6AScore models by performing PCA. This method aimed to apply the concept of dimension reduction to transform multiple indicators into a few comprehensive

indicators, whose advantage is to maintain the most important features and remove noise and insignificant features to improve data processing speed. Both principal components 1 and 2 were extracted to act as m6AScores, the method was similar to GGI (42).

$$\text{m6AScore} = \Sigma(\text{PC1}_i + \text{PC2}_i),$$

where i is the m6A prognostic-related gene expression level.

Identification of Radiomics Signatures From Digital Imaging

A total of 120 image samples matched with TCGA-BLCA samples were selected from TCIA dataset, 22 samples were excluded according to specific exclusion criteria (inadequate image quality or inability of the imaging surgeon to identify the lesion area). The study eventually included 98 samples. The constructed m6AScore model as a classifier, we extracted imaging feature from these digital images for established radiogenomic prediction models. We randomly selected 67 cases as the training dataset (46/21 = positive/negative), and the remaining 31 cases were used as an independent test dataset (21/10 = positive/negative). 98 patients were selected for a repeat region of interest (ROI) segmentation at 30 days following the initial segmentation, and this was performed by the same radiologist and an additional radiologist (6 years of experience in abdominal imaging). Then, the feature matrix was normalized. We then applied several dimensionality reduction and machine learning methods for imaging genomics model building and used the best area under the curve (AUC) value in the test group as the selection criterion to choose the best approach to construct the final model. Among them, Z-Score and Minmax normalization methods were used to normalize the data; Principal components analysis (PCA) and Pearson correlation coefficient (PCC) methods were used to pre-process the features; ANOVA, Kruskal-Wallis (KW), and Recursive feature elimination (RFE) were used to select the best features. A variety of machine learning classifiers, including SVM, LDA, logistic regression, LR-Lasso, Adaboost, Naive Bayes, and Random Forest, were used to build the radiogenomics classifier model. A total of more than a thousand models were constructed and one of them was selected as the optimal model.

Model performance was evaluated using receiver operating characteristic (ROC) curve analysis. AUC quantification was calculated. Accuracy, sensitivity, specificity, positive predictive value (PPV), and negative predictive value (NPV) were also calculated at the maximum Yorden index value of the cut-off values. We also estimated the 95% confidence intervals using 1000 samples. The above procedures were implemented using FeAture Explorer Pro (FAEPro, V 0.3.7) for Python (3.7.6).

Statistical Analysis

All statistical analyses were performed using the R software package (version 4.0.3). Differential gene expression analysis between the diverse cohorts was performed using the R package “limma.” The correlation coefficients between the m6AScore and the infiltration of immune cells were evaluated using Spearman coefficient analysis. The Kaplan-Meier method was used to plot

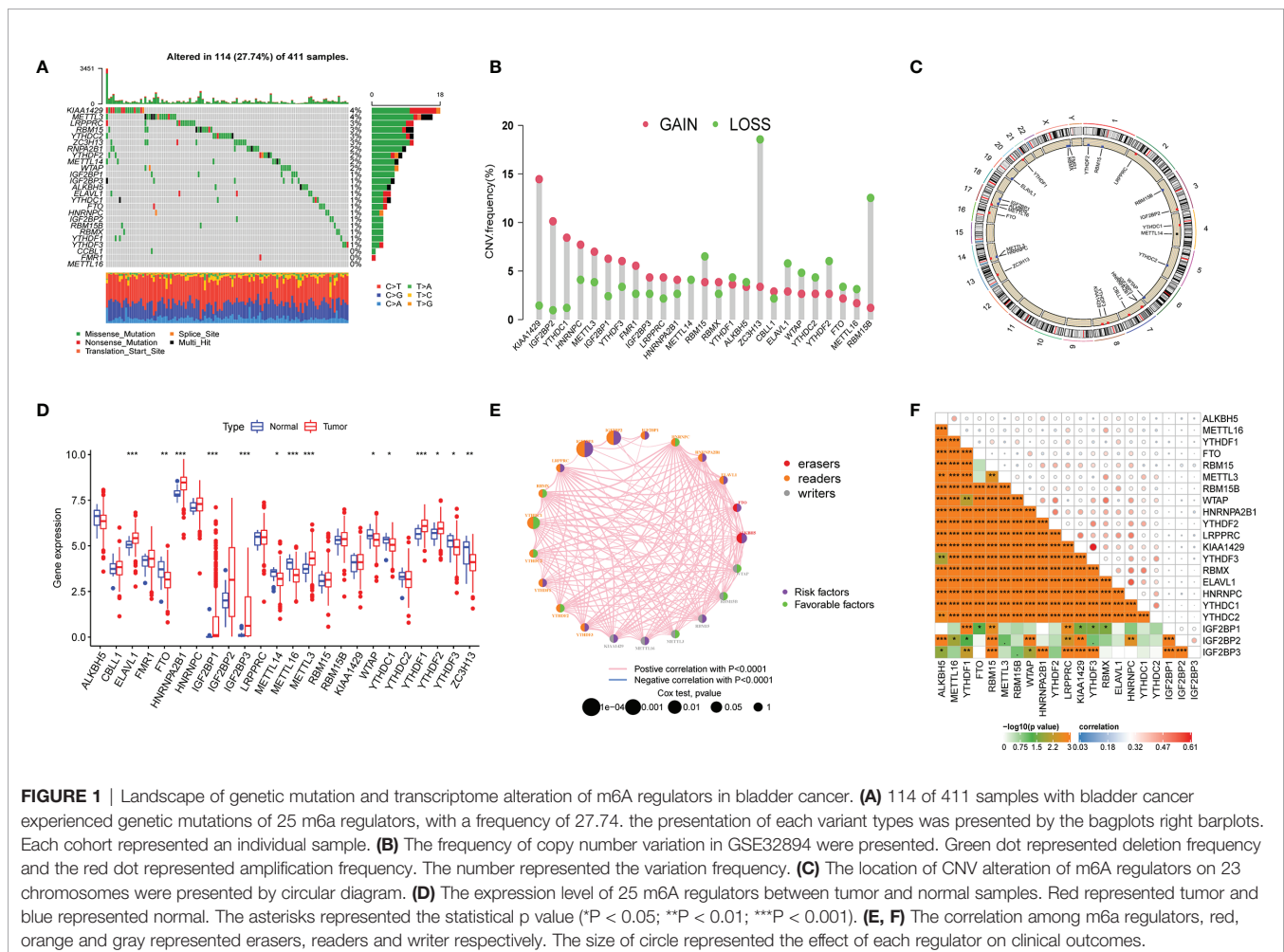
survival curves of patients with bladder cancer. AUC was used to evaluate the effective performance of constructed models using R package “pROC.” The R package “RCircos” was used to determine the location of the m6A regulators and their circular sequences along the chromosomes (43).

RESULTS

Landscape of m6A Regulators in Bladder Cancer

A total of 25 m6A regulators were collected for further analysis, including nine methyltransferases (VIRMA, WTAP, METTL3/14/15/16, RBM15, RBM15B, and ZC3H13), two demethylases (ALKBH5 and FTO), and 14 binding proteins (ELAVL1, FMR1, HNRNPA2B1, HNRNPC, IGF2BP1/2/3, LRPPRC, RBMX, YTHDC1/2, YTHDF1/2/3). We first investigated the incidence of somatic mutations and copy number variations (CNVs) of 25 m6A regulators in bladder cancer and then summarized the gene expression distribution of m6A regulators in different samples. We found that m6A regulators were altered in 114 of 411 samples (a mutation frequency of 27.74%). The waterfall plot

showed that KIAA1429 and METTL3 presented with the highest mutation frequency, mainly for missense mutations, nonsense mutations, and multiple hits, whereas METTL16 did not present as having any mutation in bladder cancer samples (Figure 1A). CNV frequency was found to be common in 25 m6A regulators of bladder cancer. We found that KIAA1429, ZC3H13, and RBM15B presented the highest CNV frequency (Figure 1B), and ZC3H13 exhibited a loss in copy number, which corresponded to the expression level of ZC3H13 in tumor samples. The location of CNV alteration of m6A regulators on 23 chromosomes is represented in a circular diagram (Figure 1C). We found that the expression levels of m6A regulators were significantly different between cancer and normal tissues (Figure 1D). The correlation and prognostic effectiveness are displayed in Figures 1E, F. We found that m6A regulators showed a significant correlation not only in the same function categories but also in diverse function categories, among writers, erasers, and binding proteins. The above analyses revealed a significant difference in expression alterations and genomic mutations in m6A regulators between cancer and normal tissues, which suggested that the m6A regulators played a vital role in tumor development.



m6AClusters Mediated by m6A Regulators

The clinical and transcriptome data of the TCGA-BLCA cohorts and GSE32894 were integrated into one meta-cohort for further analysis. The prognostic value of 21 m6A regulators was demonstrated using Kaplan–Meier (K-M) survival curves (**Supplementary Figure 1**). The results displayed that m6A regulators were significantly correlated with patients' clinical outcome. Then, unsupervised consensus clustering analysis was used to classify patients into diverse subtypes based on the expression level of the m6A regulators. Three m6AClusters were identified, including 208 samples in m6ACluster A, 308 samples in m6ACluster B, and 114 samples in m6ACluster C. Among these m6AClusters, m6ACluster B presented a significant survival advantage, while m6ACluster C exhibited the worst clinical outcome in the meta-cohort (**Figure 2A**). The PCA results also proved that the three subtypes were relatively independent of each other (**Figure 2B**). The heatmap shows the differential expression levels of m6A regulators among m6AClusters (**Figure 2C**). The expression of IGF2BP1/2/3 was significantly reduced in m6ACluster B, which revealed that IGF2BP1/2/3 may play a vital role in cancer development. GSVA was employed to investigate the biological process alteration among the three m6AClusters. The result revealed that m6ACluster A was characterized by immune activation, which enriched in toll like receptor signaling pathway, nod like receptor signaling pathway, T cell receptor signaling pathway and chemokine signaling pathway. m6ACluster B was characterized by alteration of metabolism, and m6ACluster C was significantly enriched in the cell proliferation pathway (**Figures 2D–F**).

Selection of m6A Prognostic Related Genes (MPRGs) Between Diverse Subtypes

Although the identified m6AClusters can effectively distinguish the clinical outcomes of patients with bladder cancer, the potential genetic mutations and transcriptome alterations in these subtypes are not clear. We investigated the potential m6A related genes among the diverse m6AClusters to reflect their potential effective mechanism in bladder cancer. The R package “limma” was used to select the DEGs among diverse m6AClusters, including 229 genes. (**Supplementary Figure 2**). Gene ontology (GO) enrichment analysis of these m6A related DEGs, which is summarized in **Supplementary Figure 2**, revealed that the enrichment of biological processes is significantly associated with cell proliferation and energy metabolism. These results further indicated that m6A related genes were significantly associated with tumor development. A total of 213 MPRGs were selected using univariate Cox regression analysis (**Table S1**). We applied an unsupervised clustering method to classify patients into three subtypes: gene cluster A, gene cluster B, and gene cluster C (**Figure 3A**). The K-M survival method demonstrated a significant difference among these gene subtypes; GeneCluster C presented a significant survival advantage, while GeneCluster B had the worst clinical outcome in the meta-cohort (**Figure 3B**). The expression levels of twenty-five m6A regulators in distinct

gene clusters were compared, and it was observed that the expression levels of twenty-five m6A regulators were significantly different among each gene cluster (**Figure 3E**). Furthermore, the heatmap also showed significant difference among each gene clusters in the entire transcriptome, suggesting that genomic subgroup can distinguish patients from distinct m6A methylation status. (**Figure 3D**).

Construction of m6AScore Models

Although the results of this study can predict the survival status of Bca patients, these investigations were based on the patient population and hence cannot accurately predict the m6A methylation status of an individual patient. Therefore, we constructed the m6AScore models by performing PCA according to the m6A prognostic-related gene expression levels, which could qualify the m6A methylation status of individual patients with bladder cancer. The m6AScore as well as PCA1 and PCA2 score were displayed in **Table S2**. The K-M survival method demonstrated a significant difference between the m6AScore groups; patients with a high m6AScore exhibited a significant survival advantage, while the patients with low m6AScore had the worst clinical outcomes in the meta-cohort (**Figure 3C**). At the same time, patients were classified into different cohorts according to their clinical characteristics (age, N stage, clinical stage, grade, T stage and M stage), and it was found that the m6AScore exhibited good predictive performance in the different clinical cohorts, including patients categorized by age and cancer stage (**Figure 4**). The bar plots and box plots showed that m6AScore could help distinguish between different clinical pathologies. The patients with a low m6AScore presented with a higher degree of malignancy in tumor samples, which further verified that the m6AScore had good predictive performance, predicting not only the clinical outcomes but also the clinical traits (**Supplementary Figure 3**).

Immune Cell Infiltration in m6AClusters

To explore the immune cell infiltration alteration underlying the three diverse m6AClusters, a box plot of the relative content of immune cells among the distinct subtypes was plotted by performing ssGSEA (**Figure 5A**). The results demonstrated that almost all immune cells were reduction in m6ACluster B, and increased in m6ACluster A and m6ACluster C. The immune cell infiltration was also assessed using the “ESTIMATE” algorithm, which was consistent with the results of ssGSEA that the immune score was the lowest in the m6ACluster B. (**Figure 5D**). Then stromal purity (StromalScore) and tumor cell purity (ESTIMATEScore) in the three m6AClusters were also evaluated, which displayed that StromalScore and ESTIMATEScore were increased in m6ACluster A and m6ACluster C, decrease in m6ACluster B (**Figures 5E, F**).

Prognostic Value of m6AScore

To visualize the relationship between the above models, the clinical pathology and clinical outcomes of the Sankey diagram were plotted (**Figure 6A** and **Supplementary Figure 4**). The Kruskal-Wallis test was used to better reveal the correlation

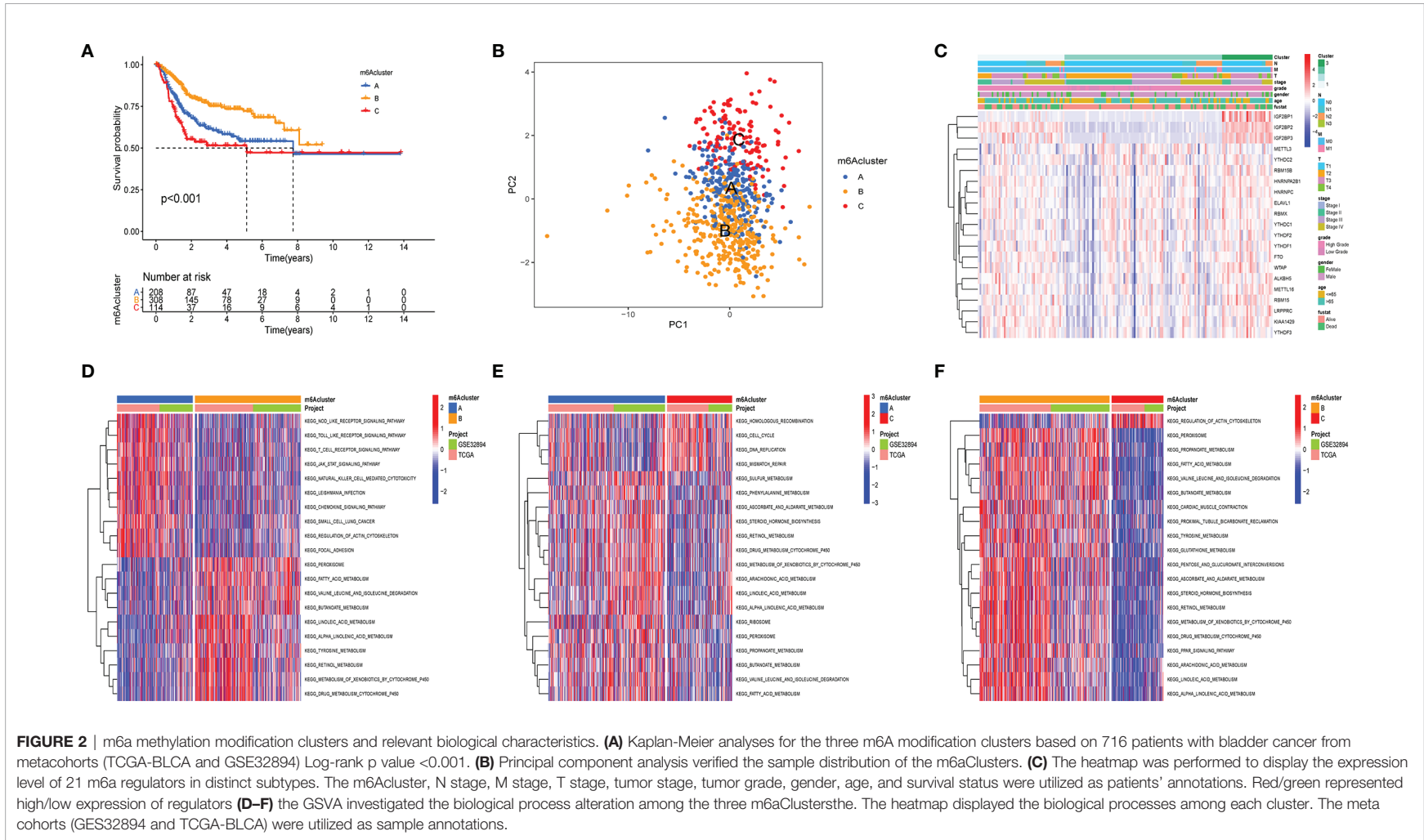
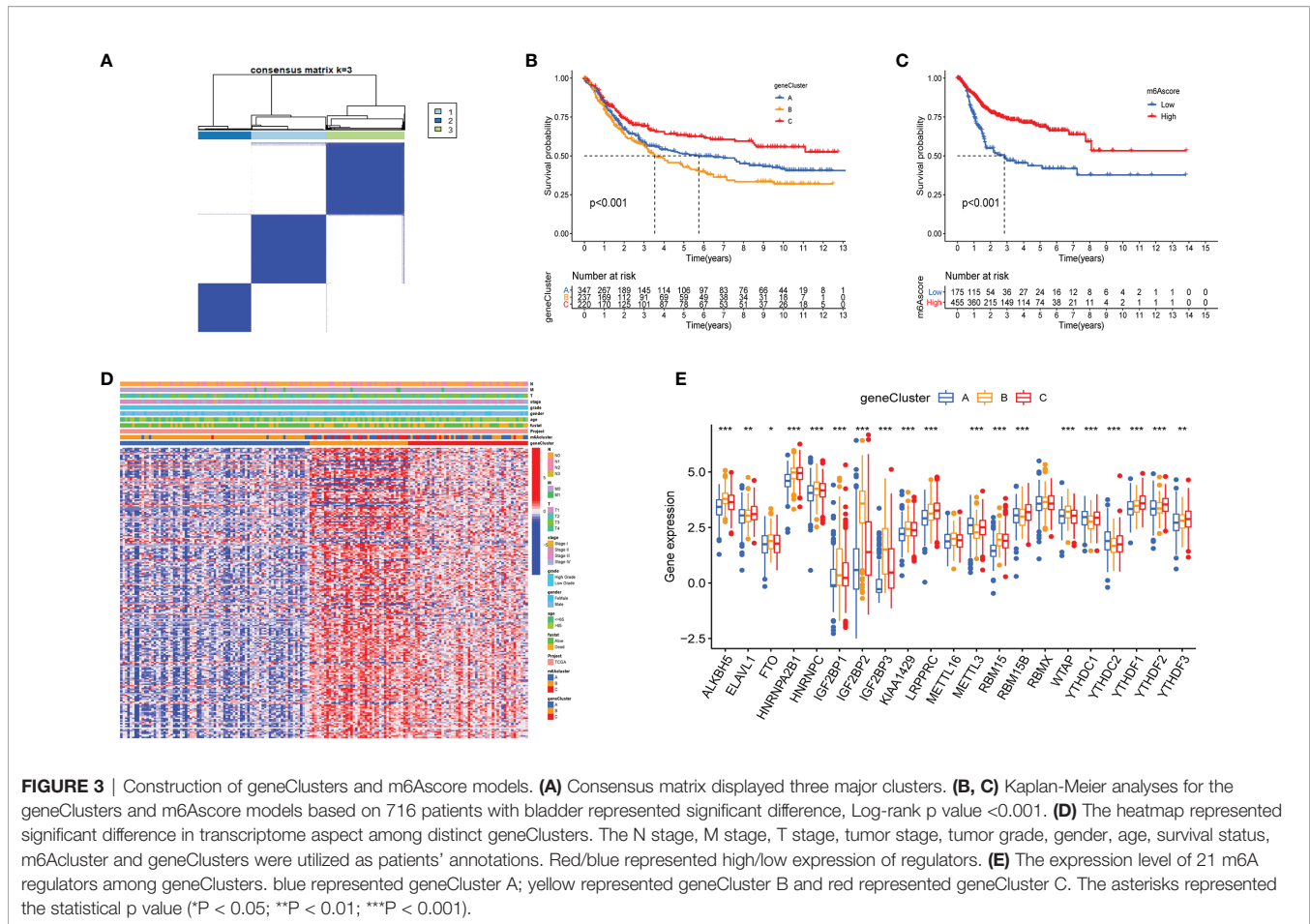


FIGURE 2 | m6a methylation modification clusters and relevant biological characteristics. **(A)** Kaplan-Meier analyses for the three m6A modification clusters based on 716 patients with bladder cancer from metacohorts (TCGA-BLCA and GSE32894) Log-rank p value <0.001. **(B)** Principal component analysis verified the sample distribution of the m6aClusters. **(C)** The heatmap was performed to display the expression level of 21 m6a regulators in distinct subtypes. The m6Acluster, N stage, M stage, T stage, tumor stage, tumor grade, gender, age, and survival status were utilized as patients' annotations. Red/green represented high/low expression of regulators **(D–F)** the GSEA investigated the biological process alteration among the three m6aClustersthe. The heatmap displayed the biological processes among each cluster. The meta cohorts (GES32894 and TCGA-BLCA) were utilized as sample annotations.



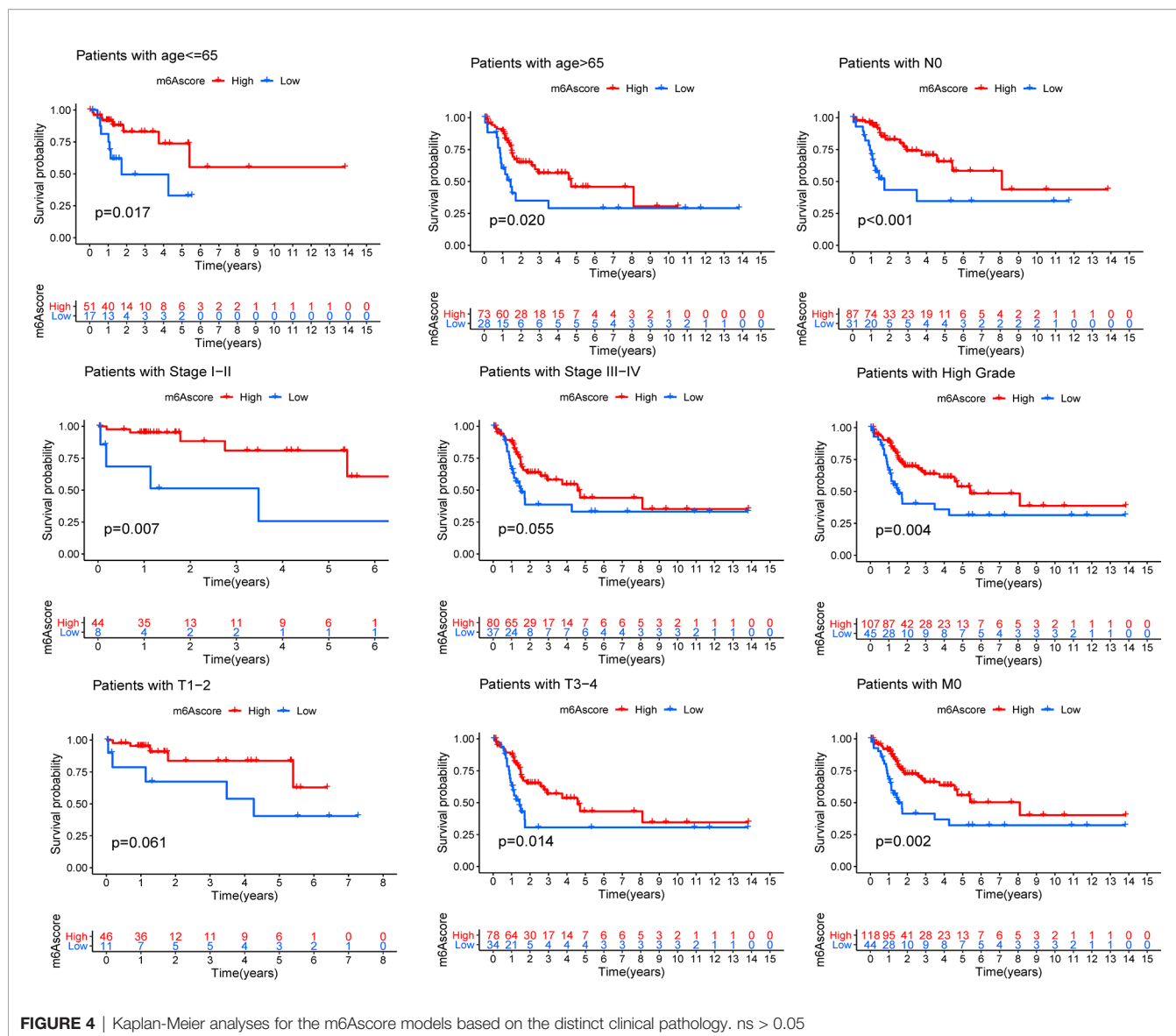
between the above models and the m6AScore. **Figure 5B** shows that m6A cluster B presented the highest median m6AScore, and **Figure 5C** shows that GeneCluster B presented the lowest median m6AScore. m6A cluster B and GeneCluster B exhibited a significant survival advantage and poor clinical outcomes, respectively, which is consistent with the prediction made using the m6AScore. Thus, these results confirmed that m6AScore could qualify the m6A methylation status of individual patients with bladder cancer.

We further analyzed the relationship between m6AScore and tumor mutational burden (TMB). The scatter diagram showed that m6AScore was significantly associated with the TMB (**Figure 6D**), and the waterfall plot also demonstrated that patients with low m6AScore presented more extensive TMB than did the patients with high m6AScore (**Figures 6B, C**). K-M analysis revealed that the patients with H-TMB exhibited a significant survival advantage, and the patients with L-TMB had the worst clinical outcomes (**Figure 6E**). To further accurately qualify the clinical status of patients with bladder cancer, we combined TMB and m6AScore to predict the clinical outcomes of each patient. K-M analysis showed that patients with H-TMB and high m6AScore exhibited a significant survival advantage, and patients with L-TMB and low m6AScore had the worst clinical outcomes (**Figure 6F**).

Besides, we observed that immune response markers such as PD1 and CTLA4 were significantly associated with the m6AScore, while patients with high m6AScore presented lower expression levels of PD1 and CTLA4 (**Supplementary Figures 3C, D**). So, we investigated whether the m6AScore could predict a patients' response to immunotherapy treatment. Our results showed that the m6AScore predicts that patients, who express CTLA4+/PD1-, respond to immunotherapy (**Supplementary Figure 3E**).

Construction of Optimal Radiomics Signatures

A total of more than a thousand models had been constructed *via* combination of several methods from each step, and the detail information of this models were displayed in **Table S3**. Using the classifier AUC values of the test group as the selection criteria for the best model, we can find that the best predictive efficacy of the imaging genomics model was achieved by a machine learning approach built with the Z-SCORE method for data normalization, the PCA method for feature pre-processing, the KW method for dimensionality reduction, and application of the LASSO-constrained logistic regression method. A comparison of the AUC values for different data pre-processing and modeling methods is shown in **Figures 7A–D**. Seven features were identified as optimal for radiomics, and the process is shown



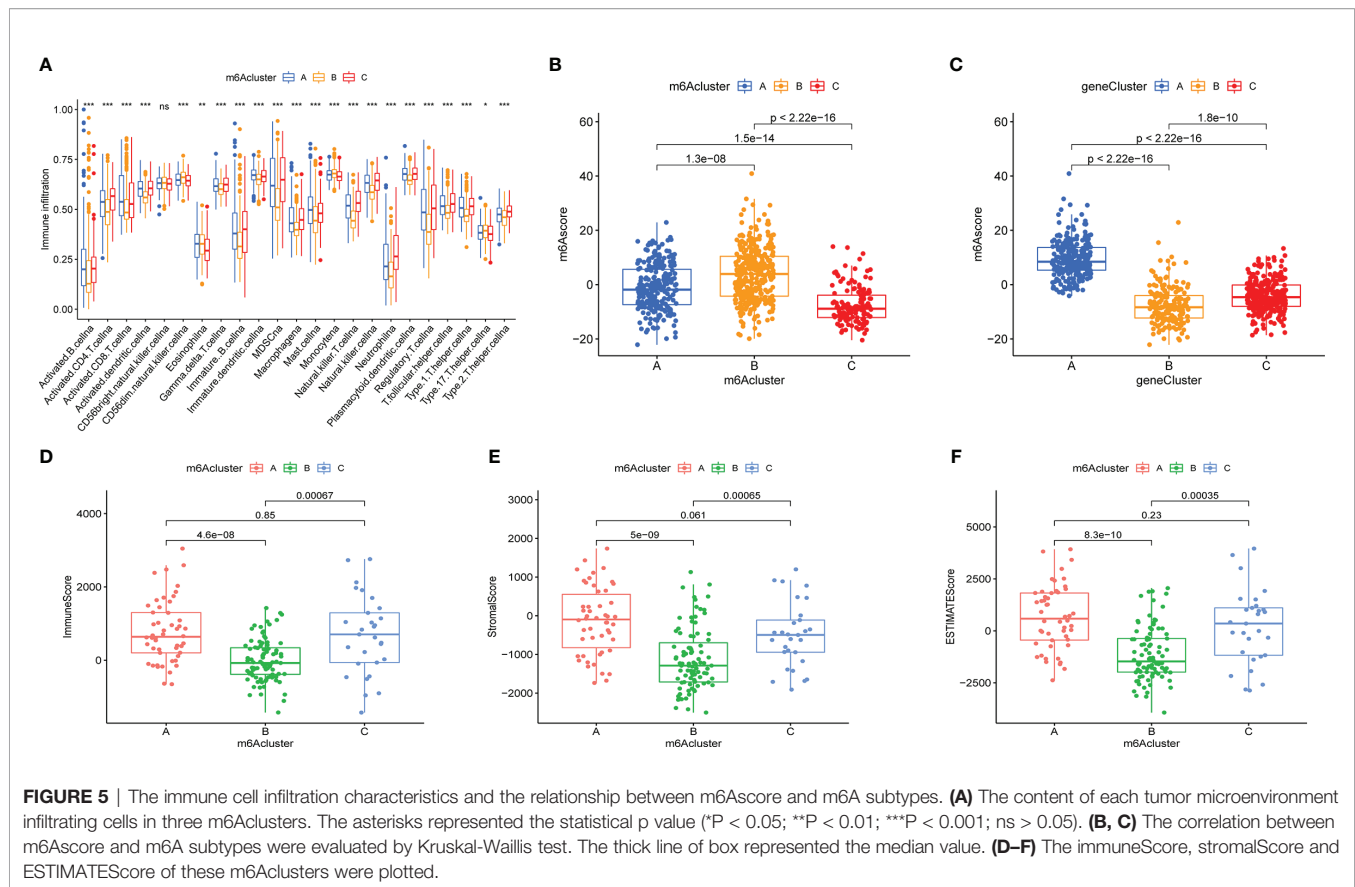
in the **Supplementary Word**. Based on these seven features, we found that the model obtained the highest AUC value for the validation dataset. At this point, the model achieved an AUC degree of 0.887 and 0.762 for the training and test datasets, respectively. The ROC curves are shown in **Figure 7F**. The selected features are shown in **Figure 7E**.

The calculation formula of the radiomics model can be seen in follow: $\text{RadScore} = 0.040 \times \text{PCA_Feature_2} - 0.103 \times \text{PCA_Feature_8} + 0.176 \times \text{PCA_Feature_19} + 0.175 \times \text{PCA_Feature_20} - 0.183 \times \text{PCA_Feature_23} + 0.297 \times \text{PCA_Feature_34} - 0.315 \times \text{PCA_Feature_57}$. The characteristics of PCA_feature was displayed in **Table S4**.

DISCUSSION

With the constant advancement in gene sequencing technology which focuses on the function and influence of reversible RNA

modification, the concept of epigenetic transcriptomics has gradually gained the attention of researchers. Due to the complexity of m6A level detection (m6A MeRIP and m6A-seq), several studies have reported alternative approaches to identify the genetic mutation of m6A regulators, and evaluated the relationship between the m6A methylation modification pattern and cancer diseases. Abnormal levels of m6A regulators have exhibited a predictive benefit in many types of cancer, such as bladder cancer (44, 45), renal clear cell carcinoma (46), prostate cancer (47, 48), and breast cancer (49). Xie et al. reported that the interaction between IGF2BP1 and circPTPRA suppresses bladder cancer progression (50). Yang et al. found that METTL3 and CDCP1 are upregulated in bladder cancer and are associated with the progression of bladder cancer (51). Jin et al. explored that m6A writer METTL3 and eraser ALKBH5 regulator cell adhesion *via* embellishing ITGA6 expression in bladder cancer (44). Xie et al. demonstrated that METTL3/YTHDF2 m6A axis degraded the



mRNA of tumor suppressors SETD7 and KLF4, contributing to the progression of bladder cancer (52). The differential expression of regulators involved in diverse tumor types provided us with a clue that the maladjustment of m6A regulators at the tissue level is complicated. Therefore, further studies on m6A regulators are required to explore the regulatory mechanism underlying m6A RNA modification in bladder cancer.

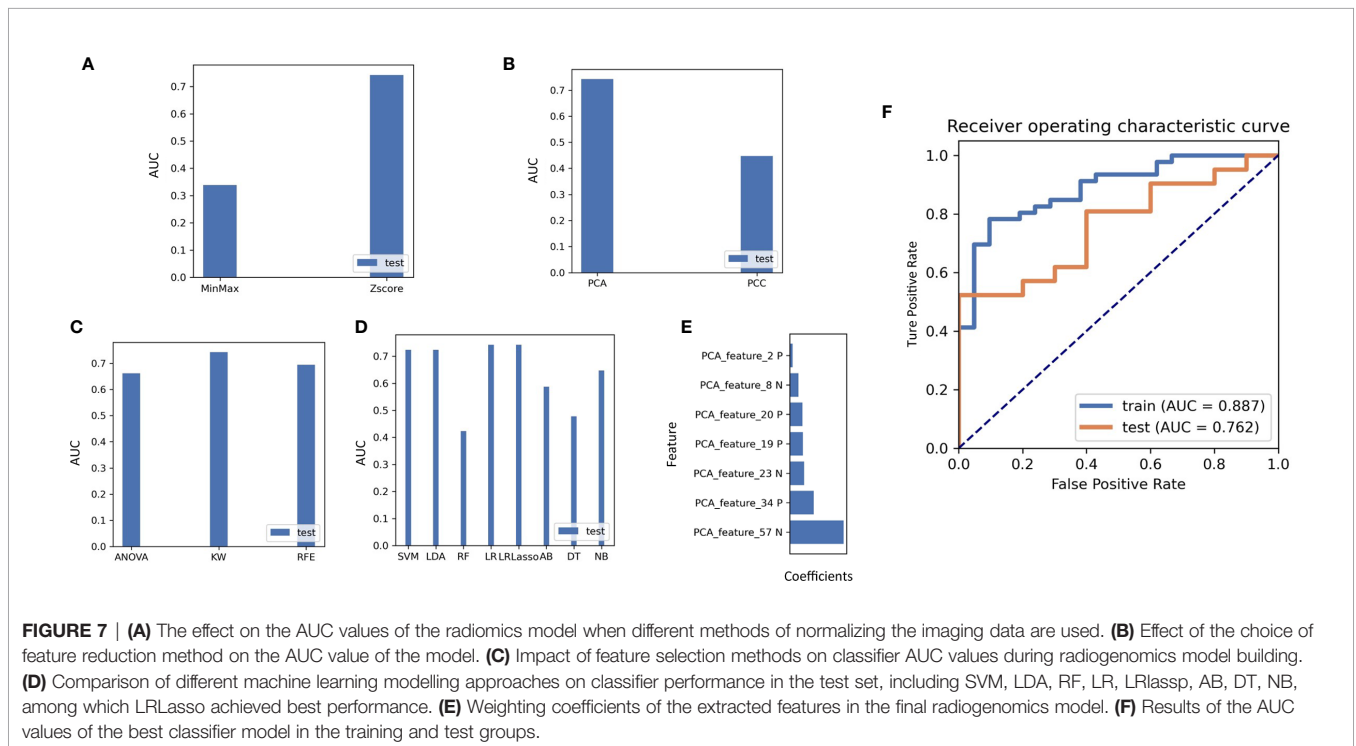
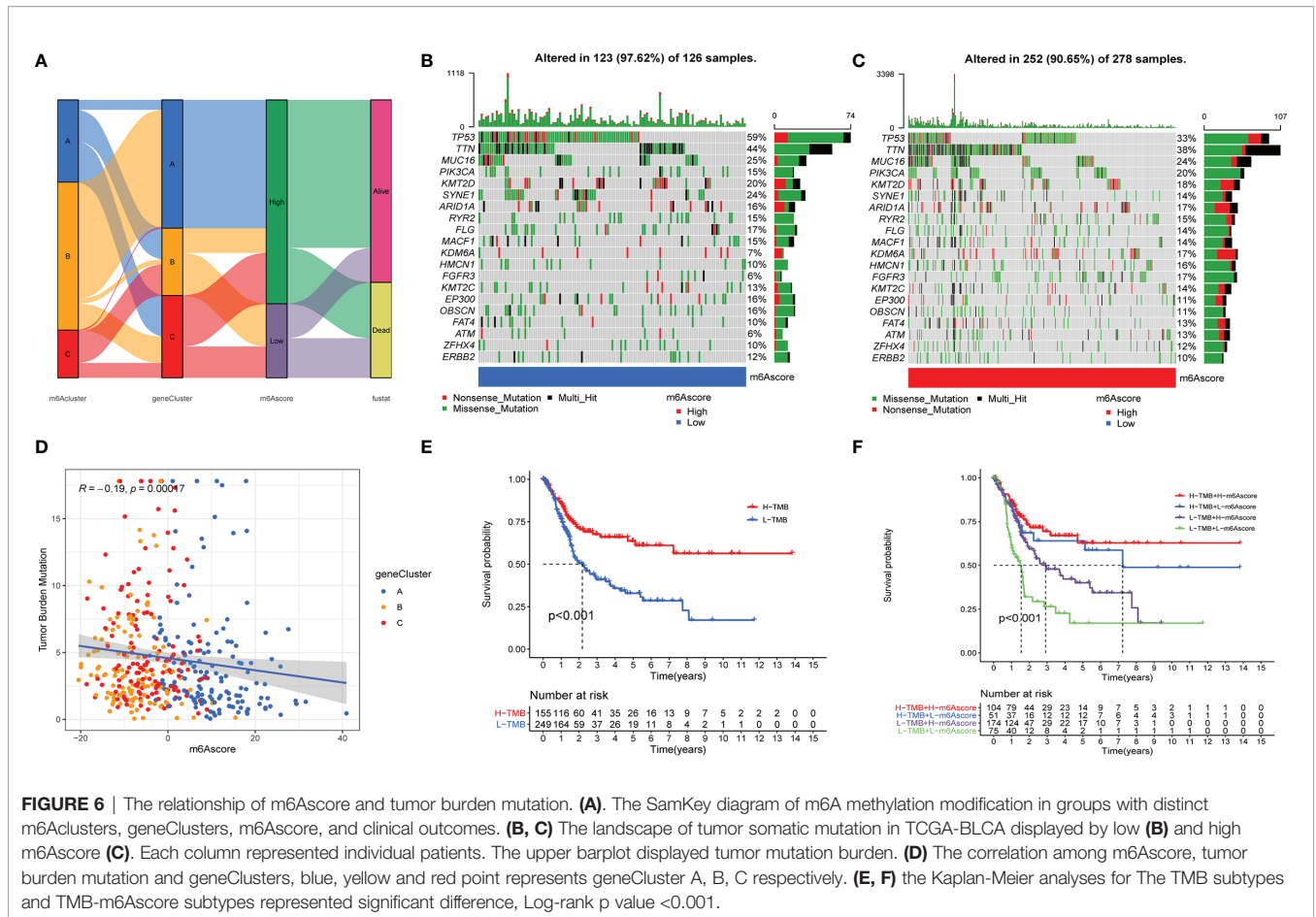
In this study, we classified bladder cancer samples into three distinct m6A methylation clusters, which can effectively predict the clinical outcome of bladder cancer, namely m6A cluster A, m6A cluster B, and m6A cluster C. We observed significant differences in immunocytes among the three m6A methylation clusters. Although the m6A cluster A and m6A cluster C were characterized by immune activation, which represented by high infiltration of activated CD8 T cells, activated B cells, nature killer cells, revealed a hot immune microenvironment, the activation of the stromal cells prevented the penetration of immune cells into the parenchyma of tumors. Therefore, it was no surprised that m6A cluster A and m6A cluster C has a poor clinical prognosis than m6A cluster B.

Beside, DEGs among these three m6A clusters were regarded as m6A methylation-related genes and might be indirectly or directly alter m6A methylation status. Then we selected m6A prognostic-related DEGs by univariate Cox regression analysis. Three transcriptome clusters were constructed according to the m6A prognostic-related factors, which were significantly

correlated with clinical outcomes. The transcriptome clusters further confirmed that these genes were related to m6A methylation status and the progression of bladder cancer.

Considering the intertumoral heterogeneity, we further constructed a quantitative model termed “m6AScore” to qualify the m6A methylation status of individual samples. In order to accurately guide the treatment of individual patients. Further analysis found that m6AScore not only can be used to predict the clinical prognosis of patients, but also can accurately distinguish between different clinical pathologies. In addition, immune response markers such as PD1 and CTLA4 were significantly related to the m6AScore, which indicated that m6AScore had the ability to assess the effective performance of immunotherapy treatment. Moreover, when combined with TMB, m6AScore has more accurate prediction performance. Therefore, these results verified m6A models may be used in clinical evaluations and targeted therapeutic schedules.

However, genomic prediction models are cumbersome and invasive, which are not conducive to auxiliary diagnosis by clinicians. Thus, we attempt to find a convenient approach to predict patients’ genetic subtype for making the appropriate clinical diagnosis. In the era of biological information digitization, radiomics analysis has been used to capture quantitative signatures from digital images that were related to the clinical pathology or molecular characteristics of patients (53). In this context, an increasing number of studies have focused on presenting genomic information on bladder cancer *via* digital imaging. For example, Wu



et al. constructed a radiomics nomogram for preoperative prediction of lymph node metastasis in bladder cancer (54). Zheng et al. evaluated the muscular invasiveness of bladder cancer by performing radiomics analysis, and the AUC was as high as 0.913 (55). In this study, AUC values as the selection criteria for identifying the best model, several methods were conducted in this research to extract the imaging features and construct radiogenomic models. It was found that the best predictive efficacy of the imaging genomics model was achieved by a machine learning approach built with the Z-SCORE method for data normalization, then the PCA method for feature pre-processing, subsequently, the KW method for dimensionality reduction, finally application of the LASSO-constrained logistic regression method for building radiogenomics classifier models. Seven features were identified as optimal for radiogenomic model. In brief, we constructed a non-invasive radiogenomic model to predict the m6a methylation status of individual patients, which may be beneficial for clinician to carry out individualized medical treatment, such as the combination of targeting m6A regulators and immunotherapy. Subsequent studies will further explore how to alter the m6a status of patients to improve the clinical prognosis.

CONCLUSION

The presented radiogenomics model, a noninvasive prediction approach that combined the radiomics signatures and genomics characteristics, displayed satisfactory effective performance for predicting survival outcomes and therapeutic responses of patients with bladder cancer. More interdisciplinary studies that combine medicine and electronic fields need to be explored.

DATA AVAILABILITY STATEMENT

Publicly available datasets were analyzed in this study. This data can be found here: <https://www.jianguoyun.com/p/DQD2zAcQh7PNCRirjPwD> and <https://portal.gdc.cancer.gov/>, with the accession number TCGA-BLCA; <https://www.ncbi.nlm.nih.gov/geo/>, with the accession number GSE32894.

REFERENCES

- Liu Q, Gregory RI. RNAmoD: An Integrated System for the Annotation of mRNA Modifications. *Nucleic Acids Res* (2019) 47(W1):W548–55. doi: 10.1093/nar/gkz479
- Chen RX, Chen X, Xia LP, Zhang JX, Pan ZZ, Ma XD, et al. N(6)-Methyladenosine Modification of Circsun2 Facilitates Cytoplasmic Export and Stabilizes HMGA2 to Promote Colorectal Liver Metastasis. *Nat Commun* (2019) 10(1):4695. doi: 10.1038/s41467-019-12651-2
- Ni W, Yao S, Zhou Y, Liu Y, Huang P, Zhou A, et al. Long Noncoding RNA GAS5 Inhibits Progression of Colorectal Cancer by Interacting With and Triggering YAP Phosphorylation and Degradation and Is Negatively Regulated by the M(6)A Reader YTHDF3. *Mol Cancer* (2019) 18(1):143. doi: 10.1186/s12943-019-1079-y
- Kasowitz SD, Ma J, Anderson SJ, Leu NA, Xu Y, Gregory BD, et al. Nuclear M6a Reader YTHDC1 Regulates Alternative Polyadenylation and Splicing During Mouse Oocyte Development. *PLoS Genet* (2018) 14(5):e1007412. doi: 10.1371/journal.pgen.1007412
- Tang C, Klukovich R, Peng H, Wang Z, Yu T, Zhang Y, et al. ALKBH5-Dependent M6a Demethylation Controls Splicing and Stability of Long 3'-

AUTHOR CONTRIBUTIONS

FY, YH, and JG contributed equally to this work. FY and JG designed and conceptualized the study. HJ supervised the study. All authors contributed toward data collection and analysis.

FUNDING

This study was supported by the National Natural Science Foundation of China (Grant Numbers: 81872102).

ACKNOWLEDGMENTS

We sincerely appreciate all members who participated in data collection and analysis.

SUPPLEMENTARY MATERIAL

The Supplementary Material for this article can be found online at: <https://www.frontiersin.org/articles/10.3389/fimmu.2021.722642/full#supplementary-material>

Supplementary Figure S1 | The prognostic value of twenty-five m6a regulators were displayed via K-M survival curves.

Supplementary Figure S2 | The bar and box chart of m6A score in groups with distinct tumor grade, tumor stage, T stage, and clinical outcomes.

Supplementary Figure S3 | (A) The venn diagram displayed 229 overlapping genes were selected among m6Aclusters (B) The top 10 enriched GO terms including (BP, CC and MF). (C, D) validation of the CTLA4 and the PD-L1 expression level in low and high-m6Ascore group. (E) Validation of the immune response in low and high-m6Ascore group.

Supplementary Figure S4 | The SamKey diagram of m6A methylation modification in groups with distinct m6Aclusters, geneClusters, m6Ascore, and clinical outcomes.

- UTR mRNAs in Male Germ Cells. *Proc Natl Acad Sci USA* (2018) 115(2):E325–33. doi: 10.1073/pnas.1717794115
- Zeng C, Huang W, Li Y, Weng H. Roles of METTL3 in Cancer: Mechanisms and Therapeutic Targeting. *J Hematol Oncol* (2020) 13(1):117. doi: 10.1186/s13045-020-00951-w
 - Lin S, Choe J, Du P, Triboulet R, Gregory RI. The M(6)A Methyltransferase METTL3 Promotes Translation in Human Cancer Cells. *Mol Cell* (2016) 62(3):335–45. doi: 10.1016/j.molcel.2016.03.021
 - Huang Y, Yan J, Li Q, Li J, Gong S, Zhou H, et al. Meclofenamic Acid Selectively Inhibits FTO Demethylation of M6a Over ALKBH5. *Nucleic Acids Res* (2015) 43(1):373–84. doi: 10.1093/nar/gku1276
 - Guo X, Li K, Jiang W, Hu Y, Xiao W, Huang Y, et al. RNA Demethylase ALKBH5 Prevents Pancreatic Cancer Progression by Posttranscriptional Activation of PER1 in an M6a-YTHDF2-Dependent Manner. *Mol Cancer* (2020) 19(1):91. doi: 10.1186/s12943-020-01158-w
 - Chen Y, Peng C, Chen J, Chen D, Yang B, He B, et al. WTAP Facilitates Progression of Hepatocellular Carcinoma via M6a-HuR-Dependent Epigenetic Silencing of ETS1. *Mol Cancer* (2019) 18(1):127. doi: 10.1186/s12943-019-1053-8

11. Arguello AE, DeLiberto AN, Kleiner RE. RNA Chemical Proteomics Reveals the N(6)-Methyladenosine (M(6)A)-Regulated Protein-RNA Interactome. *J Am Chem Soc* (2017) 139(48):17249–52. doi: 10.1021/jacs.7b09213
12. Bertero A, Brown S, Madrigal P, Osnato A, Ortman D, Yiangou L, et al. The SMAD2/3 Interactome Reveals That Tgfb Controls M(6)A mRNA Methylation in Pluripotency. *Nature* (2018) 555(7695):256–9. doi: 10.1038/nature25784
13. Han J, Wang JZ, Yang X, Yu H, Zhou R, Lu HC, et al. METTL3 Promote Tumor Proliferation of Bladder Cancer by Accelerating Pri-Mir221/222 Maturation in M6a-Dependent Manner. *Mol Cancer* (2019) 18(1):110. doi: 10.1186/s12943-019-1036-9
14. Zhang C, Huang S, Zhuang H, Ruan S, Zhou Z, Huang K, et al. YTHDF2 Promotes the Liver Cancer Stem Cell Phenotype and Cancer Metastasis by Regulating OCT4 Expression via M6a RNA Methylation. *Oncogene* (2020) 39(23):4507–18. doi: 10.1038/s41388-020-1303-7
15. Geng Y, Guan R, Hong W, Huang B, Liu P, Guo X, et al. Identification of M6a-Related Genes and M6a RNA Methylation Regulators in Pancreatic Cancer and Their Association With Survival. *Ann Transl Med* (2020) 8(6):387. doi: 10.21037/atm.2020.03.98
16. Ji L, Chen S, Gu L, Zhang X. Exploration of Potential Roles of M6a Regulators in Colorectal Cancer Prognosis. *Front Oncol* (2020) 10:768. doi: 10.3389/fonc.2020.00768
17. Yu H, Yang X, Tang J, Si S, Zhou Z, Lu J, et al. ALKBH5 Inhibited Cell Proliferation and Sensitized Bladder Cancer Cells to Cisplatin by M6a-CK2 α -Mediated Glycolysis. *Mol Ther Nucleic Acids* (2021) 23:27–41. doi: 10.1016/j.omtn.2020.10.031
18. Shen X, Hu B, Xu J, Qin W, Fu Y, Wang S, et al. The M6a Methylation Landscape Stratifies Hepatocellular Carcinoma Into 3 Subtypes With Distinct Metabolic Characteristics. *Cancer Biol Med* (2020) 17(4):937–52. doi: 10.20892/j.issn.2095-3941.2020.0402
19. Kocak B, Durmaz ES, Ates E, Sel I, Turgut Gunes S, Kaya OK, et al. Radiogenomics of Lower-Grade Gliomas: Machine Learning-Based MRI Texture Analysis for Predicting 1p/19q Codeletion Status. *Eur Radiol* (2020) 30(2):877–86. doi: 10.1007/s00330-019-06492-2
20. Huang YQ, Liang CH, He L, Tian J, Liang CS, Chen X, et al. Development and Validation of a Radiomics Nomogram for Preoperative Prediction of Lymph Node Metastasis in Colorectal Cancer. *J Clin Oncol* (2016) 34(18):2157–64. doi: 10.1200/JCO.2015.65.9128
21. Zhang B, Tian J, Dong D, Gu D, Dong Y, Zhang L, et al. Radiomics Features of Multiparametric MRI as Novel Prognostic Factors in Advanced Nasopharyngeal Carcinoma. *Clin Cancer Res* (2017) 23(15):4259–69. doi: 10.1158/1078-0432.CCR-16-2910
22. Beer L, Sahin H, Bateman NW, Blazic I, Vargas HA, Veeraraghavan H, et al. Integration of Proteomics With CT-Based Qualitative and Radiomic Features in High-Grade Serous Ovarian Cancer Patients: An Exploratory Analysis. *Eur Radiol* (2020) 30(8):4306–16. doi: 10.1007/s00330-020-06755-3
23. Lopez CJ, Nagornaya N, Parra NA, Kwon D, Ishkanian F, Markoe AM, et al. Association of Radiomics and Metabolic Tumor Volumes in Radiation Treatment of Glioblastoma Multiforme. *Int J Radiat Oncol Biol Phys* (2017) 97(3):586–95. doi: 10.1016/j.ijrobp.2016.11.011
24. Kim M, Jung SY, Park JE, Jo Y, Park SY, Nam SJ, et al. Diffusion- and Perfusion-Weighted MRI Radiomics Model May Predict Isocitrate Dehydrogenase (IDH) Mutation and Tumor Aggressiveness in Diffuse Lower Grade Glioma. *Eur Radiol* (2020) 30(4):2142–51. doi: 10.1007/s00330-019-06548-3
25. Zhang J, Zhao X, Zhao Y, Zhang J, Zhang Z, Wang J, et al. Value of Pre-Therapy (18)F-FDG PET/CT Radiomics in Predicting EGFR Mutation Status in Patients With Non-Small Cell Lung Cancer. *Eur J Nucl Med Mol Imaging* (2020) 47(5):1137–46. doi: 10.1007/s00259-019-04592-1
26. Wei J, Yang G, Hao X, Gu D, Tan Y, Wang X, et al. A Multi-Sequence and Habitat-Based MRI Radiomics Signature for Preoperative Prediction of MGMT Promoter Methylation in Astrocytomas With Prognostic Implication. *Eur Radiol* (2019) 29(2):877–88. doi: 10.1007/s00330-018-5575-z
27. Yang L, Gu D, Wei J, Yang C, Rao S, Wang W, et al. A Radiomics Nomogram for Preoperative Prediction of Microvascular Invasion in Hepatocellular Carcinoma. *Liver Cancer* (2019) 8(5):373–86. doi: 10.1159/000494099
28. Hu LS, Ning S, Eschbacher JM, Baxter LC, Gaw N, Ranjbar S, et al. Radiogenomics to Characterize Regional Genetic Heterogeneity in Glioblastoma. *Neuro Oncol* (2017) 19(1):128–37. doi: 10.1093/neuonc/now135
29. Siegel RL, Miller KD, Fuchs HE, Jemal A. Cancer Statistics, 2021. *CA Cancer J Clin* (2021) 71(1):7–33. doi: 10.3322/caac.21654
30. Craig AJ, von Felden J, Garcia-Lezana T, Sarcognato S, Villanueva A. Tumour Evolution in Hepatocellular Carcinoma. *Nat Rev Gastroenterol Hepatol* (2020) 17(3):139–52. doi: 10.1038/s41575-019-0229-4
31. Qiu Z, Li H, Zhang Z, Zhu Z, He S, Wang X, et al. A Pharmacogenomic Landscape in Human Liver Cancers. *Cancer Cell* (2019) 36(2):179–93.e11. doi: 10.1016/j.ccell.2019.07.001
32. Xu X, Wang H, Guo Y, Zhang X, Li B, Du P, et al. Study Progress of Noninvasive Imaging and Radiomics for Decoding the Phenotypes and Recurrence Risk of Bladder Cancer. *Front Oncol* (2021) 11:704039. doi: 10.3389/fonc.2021.704039
33. Xu S, Yao Q, Liu G, Jin D, Chen H, Xu J, et al. Combining DWI Radiomics Features With Transurethral Resection Promotes the Differentiation Between Muscle-Invasive Bladder Cancer and Non-Muscle-Invasive Bladder Cancer. *Eur Radiol* (2020) 30(3):1804–12. doi: 10.1007/s00330-019-06484-2
34. Ma S, Chen C, Ji X, Liu J, Zhou Q, Wang G, et al. The Interplay Between M6a RNA Methylation and Noncoding RNA in Cancer. *J Hematol Oncol* (2019) 12(1):121. doi: 10.1186/s13045-019-0805-7
35. Chen M, Wong CM. The Emerging Roles of N6-Methyladenosine (M6a) Deregulation in Liver Carcinogenesis. *Mol Cancer* (2020) 19(1):44. doi: 10.1186/s12943-020-01172-y
36. He L, Li H, Wu A, Peng Y, Shu G, Yin G. Functions of N6-Methyladenosine and Its Role in Cancer. *Mol Cancer* (2019) 18(1):176. doi: 10.1186/s12943-019-1109-9
37. Wang T, Kong S, Tao M, Ju S. The Potential Role of RNA N6-Methyladenosine in Cancer Progression. *Mol Cancer* (2020) 19(1):88. doi: 10.1186/s12943-020-01204-7
38. Hänzelmann S, Castelo R, Guinney J. GSEA: Gene Set Variation Analysis for Microarray and RNA-Seq Data. *BMC Bioinf* (2013) 14:7. doi: 10.1186/1471-2105-14-7
39. Mariathan S, Turley SJ, Nickles D, Castiglioni A, Yuen K, Wang Y, et al. Tgfb Attenuates Tumour Response to PD-L1 Blockade by Contributing to Exclusion of T Cells. *Nature* (2018) 554(7693):544–8. doi: 10.1038/nature25501
40. Barbie DA, Tamayo P, Boehm JS, Kim SY, Moody SE, Dunn IF, et al. Systemic RNA Interference Reveals That Oncogenic KRAS-Driven Cancers Require TBK1. *Nature* (2009) 462(7269):108–12. doi: 10.1038/nature08460
41. Xue Y, Tong L, LiuAnwei Liu F, Liu A, Zeng S, Xiong Q, et al. Tumor -infiltrating M2 Macrophages Driven by Specific Genomic Alterations Are Associated With Prognosis in Bladder Cancer. *Oncol Rep* (2019) 42(2):581–94. doi: 10.3892/or.2019.7196
42. Sotiriou C, Wirapati P, Loi S, Harris A, Fox S, Smeds J, et al. Gene Expression Profiling in Breast Cancer: Understanding the Molecular Basis of Histologic Grade to Improve Prognosis. *J Natl Cancer Inst* (2006) 98(4):262–72. doi: 10.1093/jnci/dij052
43. Mayakonda A, Lin DC, Assenov Y, Plass C, Koeffler HP. Maftools: Efficient and Comprehensive Analysis of Somatic Variants in Cancer. *Genome Res* (2018) 28(11):1747–56. doi: 10.1101/gr.239244.118
44. Jin H, Ying X, Que B, Wang X, Chao Y, Zhang H, et al. N(6)-Methyladenosine Modification of ITGA6 mRNA Promotes the Development and Progression of Bladder Cancer. *EBioMedicine* (2019) 47:195–207. doi: 10.1016/j.jebiom.2019.07.068
45. Cheng M, Sheng L, Gao Q, Xiong Q, Zhang H, Wu M, et al. The M(6)A Methyltransferase METTL3 Promotes Bladder Cancer Progression via AFF4/NF-kb/MYC Signaling Network. *Oncogene* (2019) 38(19):3667–80. doi: 10.1038/s41388-019-0683-z
46. Zhang QJ, Luan JC, Song LB, Cong R, Ji CJ, Zhou X, et al. M6a RNA Methylation Regulators Correlate With Malignant Progression and Have Potential Predictive Values in Clear Cell Renal Cell Carcinoma. *Exp Cell Res* (2020) 392(1):112015. doi: 10.1016/j.yexcr.2020.112015
47. Du C, Lv C, Feng Y, Yu S. Activation of the KDM5A/miRNA-495/YTHDF2/m6A-MOB3B Axis Facilitates Prostate Cancer Progression. *J Exp Clin Cancer Res* (2020) 39(1):223. doi: 10.1186/s13046-020-01735-3
48. Barros-Silva D, Lobo J, Guimarães-Teixeira C, Carneiro I, Oliveira J, Martens-Uzunova ES, et al. VIRMA-Dependent N6-Methyladenosine Modifications Regulate the Expression of Long Non-Coding RNAs CCAT1

- and CCAT2 in Prostate Cancer. *Cancers (Basel)* (2020) 12(4):771. doi: 10.3390/cancers12040771
49. Zhang C, Samanta D, Lu H, Bullen JW, Zhang H, Chen I, et al. Hypoxia Induces the Breast Cancer Stem Cell Phenotype by HIF-Dependent and ALKBH5-Mediated M⁶A-Demethylation of NANOG mRNA. *Proc Natl Acad Sci USA* (2016) 113(14):E2047–56. doi: 10.1073/pnas.1602883113
50. Xie F, Huang C, Liu F, Zhang H, Xiao X, Sun J, et al. CircPTPRA Blocks the Recognition of RNA N(6)-Methyladenosine Through Interacting With IGF2BP1 to Suppress Bladder Cancer Progression. *Mol Cancer* (2021) 20(1):68. doi: 10.1186/s12943-021-01359-x
51. Yang F, Jin H, Que B, Chao Y, Zhang H, Ying X, et al. Dynamic M(6)A mRNA Methylation Reveals the Role of METTL3-M(6)A-CDCP1 Signaling Axis in Chemical Carcinogenesis. *Oncogene* (2019) 38(24):4755–72. doi: 10.1038/s41388-019-0755-0
52. Xie H, Li J, Ying Y, Yan H, Jin K, Ma X, et al. METTL3/YTHDF2 M(6) A Axis Promotes Tumorigenesis by Degrading SETD7 and KLF4 mRNAs in Bladder Cancer. *J Cell Mol Med* (2020) 24(7):4092–104. doi: 10.1111/jcmm.15063
53. Mayerhoefer ME, Materka A, Langs G, Häggström I, Szczypiński P, Gibbs P, et al. Introduction to Radiomics. *J Nucl Med* (2020) 61(4):488–95. doi: 10.2967/jnumed.118.222893
54. Wu S, Zheng J, Li Y, Yu H, Shi S, Xie W, et al. A Radiomics Nomogram for the Preoperative Prediction of Lymph Node Metastasis in Bladder Cancer. *Clin Cancer Res* (2017) 23(22):6904–11. doi: 10.1158/1078-0432.CCR-17-1510
55. Zheng J, Kong J, Wu S, Li Y, Cai J, Yu H, et al. Development of a Noninvasive Tool to Preoperatively Evaluate the Muscular Invasiveness of Bladder Cancer Using a Radiomics Approach. *Cancer* (2019) 125(24):4388–98. doi: 10.1002/cncr.32490

Conflict of Interest: The authors declare that this research was conducted in the absence of any commercial or financial relationships that could be construed as a potential conflict of interest.

Publisher's Note: All claims expressed in this article are solely those of the authors and do not necessarily represent those of their affiliated organizations, or those of the publisher, the editors and the reviewers. Any product that may be evaluated in this article, or claim that may be made by its manufacturer, is not guaranteed or endorsed by the publisher.

Copyright © 2021 Ye, Hu, Gao, Liang, Liu, Ou, Cheng and Jiang. This is an open-access article distributed under the terms of the Creative Commons Attribution License (CC BY). The use, distribution or reproduction in other forums is permitted, provided the original author(s) and the copyright owner(s) are credited and that the original publication in this journal is cited, in accordance with accepted academic practice. No use, distribution or reproduction is permitted which does not comply with these terms.